



Research article

Na⁺_i/K⁺_i imbalance contributes to gene expression in endothelial cells exposed to elevated NaCl

D.A. Fedorov^a, S.V. Sidorenko^a, A.I. Yusipovich^a, E.Y. Parshina^a, A.M. Tverskoi^{a,b}, P.A. Abramicheva^a, G.V. Maksimov^a, S.N. Orlov^a, O.D. Lopina^a, E.A. Klimanova^{a,*}^a Faculty of Biology, Lomonosov Moscow State University, Moscow, 1-12 Leninskie Gory, 119234, Russia^b Engelhardt Institute of Molecular Biology, Russian Academy of Sciences, Moscow, 32 Vavilova Street, 119991, Russia

ARTICLE INFO

Keywords:

Sodium
Osmolarity
Inflammation
Endothelium
Hypertension

ABSTRACT

High-salt consumption contributes to the development of hypertension and is considered an independent risk factor for vascular remodelling, cardiac hypertrophy and stroke incidence. Alterations in NO production, inflammation and endothelial cell stiffening are considered now as plausible mediators of cardiovascular dysfunction. We studied early responses of endothelial cells (HUVEC) caused by a moderate increase in extracellular sodium concentration. Exposure of HUVEC to elevated sodium within the physiological range up to 24 h is accompanied by changes in monovalent cations fluxes and Na,K-ATPase activation, and, in turn, results in a significant decrease in the content of *PTGS2*, *IL6* and *IL1LR1* mRNAs. The expression of *NOS3* and *FOS* genes, as well as the abundance of cytosolic and nuclear NFAT5 protein, remained unchanged. We assessed the mechanical properties of endothelial cells by estimating Young's modulus and equivalent elastic constant using atomic force and interference microscopy, respectively. These parameters were unaffected by elevated-salt exposure for 24 h. The data obtained suggest that even small and short-term elevations of extracellular sodium concentration affect the expression of genes involved in the control of endothelial function through the Na⁺_i/K⁺_i-dependent mechanism(s).

1. Introduction

Numerous epidemiological and intervention studies have demonstrated a positive correlation between salt intake, endothelial dysfunction and elevated blood pressure (Dickinson et al. 2011). High-salt consumption has also been shown to be associated with other disorders including diabetes mellitus, preeclampsia, and autoimmune diseases (Oh et al., 2016). Despite the obvious pathophysiological consequences, the early response to high salt load, leading later to the development of endothelial and vascular dysfunction, remains poorly investigated. *A priori*, high-salt intake may contribute to the development of above-listed disorders via signals triggered by augmented concentration of extracellular sodium ([Na⁺]_o), chloride ([Cl⁻]_o) and/or osmolarity of the extracellular fluids determined by combined elevation of [Na⁺]_o and [Cl⁻]_o.

There is a lot of evidence that high salt treatment of various types of cells provokes their acquisition of a pro-inflammatory phenotype (Wenzel et al., 2019). In this respect, endothelial cells have been most studied, however, the mechanism of the pathogenic effect of high-salt treatment

on its function and metabolism remains poorly understood. The endothelium lining the vascular walls is directly exposed to blood plasma, where the [Na⁺]_o is usually from 128 to 140 mM (Aramburu and López-Rodríguez 2019). This parameter is strictly regulated, and typically does not exceed 5% even with a sharp modulation of salt intake (Wardener et al., 2004). However, even minor changes in the extracellular sodium concentration can affect cell metabolism. Indeed, excess salt has been shown to reduce NO production by endothelial cells (H. E. de Wardener et al., 2007), augment the expression of pro-inflammatory factors (Dmitrieva and Burg 2015), and increase endothelial-monocytic cell interactions (Wild et al., 2014).

Endothelium has an extensive glycocalyx, the main part of which is a network of glycosaminoglycans that store sodium ions (Hans Oberleithner and Wilhelm, 2015). It has been shown that an excess of consumed sodium is deposited in the form of an osmotically inactive cation in some tissues, in the cells of which negatively charged glycosaminoglycans are abundantly represented (e.g., skin and muscles) (Minegishi et al., 2020). In some conditions (e.g., type 1 diabetes, chronic kidney disease), a

* Corresponding author.

E-mail address: klimanova.ea@yandex.ru (E.A. Klimanova).

disturbance of the glycocalyx integrity is observed, which is accompanied by the release of osmotically active sodium and leads to a change in the local extracellular $[Na^+]_o$ (Olde Engberink et al., 2017). It is believed that the key components of the “elevated extracellular NaCl – endothelial response” system are augmented cell stiffness (Fels et al., 2014) and NFAT5 (Nuclear factor of activated T-cells 5)-dependent osmotic sensitivity (Dmitrieva and Burg 2014). Thus, it was shown that excess sodium damages the vascular glycocalyx and stiffens endothelial cell (Hans Oberleithner and Wilhelmi 2015), that, in turn, affects gene transcription (Charbonier et al. 2019). It should be noted that endothelial cell stiffness is more dependent on sodium concentration than on the osmolarity (H. Oberleithner et al., 2009). The regulation of NFAT5, on the contrary, is sodium-independent and is sensitive to changes in the tonicity of the medium (Woo et al., 2000).

Our previous studies strongly suggest that Na^+_i/K^+_i imbalance itself can trigger subsequent transcriptomic changes in various types of cells through Ca^{2+} -independent mechanism(s) (Koltsova et al., 2012; Sidorenko et al., 2018). These data allowed us to propose that even minor and short-term elevation in the extracellular $[Na^+]_o$ may control endothelial function directly via Na^+_i/K^+_i -dependent genes expression. The present study supports this hypothesis.

2. Materials and methods

2.1. Materials

RbCl was obtained from Chem-Impex (#07221, Illinois, Wood Dale, IL, USA). TCA (#BP555), ECL kit (#34096), Trizol reagent (#15596026), 100X Halt™ phosphatase inhibitor Cocktail (#78420), RIPA buffer (#89900) were from ThermoFisher Scientific (Massachusetts, Waltham, MA, USA). NaCl (#194848) and KCl (#194844) was obtained from MP Biomedicals (Ohio, Solon, OH, USA). Mannitol was from AppliChem (#142067.1210, Darmstadt, Germany). HEPES was obtained from Flow Laboratories (#15-884-15, California, Hyland Ave Costa Mesa, CA, USA). $MgCl_2$ was purchased from Honeywell (#63020, Charlotte, North Carolina, USA). Nonidet P-40 was obtained from Helicon (Am-E109, Moscow, Russia). Secondary anti-rabbit HRP-conjugated antibodies (#AP132P) were obtained from Millipore (California, Temecula, CA, USA). Quick-RNA MicroPrep microkit columns was obtained from Zymo Research (#R1051, California, Irvine, CA, USA). The ImProm-ITM Reverse Transcription System kit was obtained from Promega, (#A3800, Wisconsin, Madison, WI, USA). QIAquick Gel Extraction Kit was obtained from Qiagen (#28704, Maryland, Germantown, MD, USA). Unless otherwise noted, all chemicals were of the purest grade.

2.2. Cell culture

Human umbilical vein endothelial cells (HUVEC) were purchased from Cell Applications (#200-05n, California, San-Diego, CA, USA) and passaged up to 4 times. Cells were seeded at a density of $\sim 2 \times 10^4$ cell per well in 6-well plates containing endothelial cell growth medium (#211-500, Cell Applications, California, San-Diego, CA, USA) and kept at 37 °C in a humidified atmosphere with 5% CO_2 /balance air. Culture cell medium was changed every 48 h. Five-seven days after plating, the cells had reached 80–85% confluence and were incubated in the presence of normal (standard cell culture medium containing approximately 125 mM Na^+) or elevated (additional 15 mM NaCl on top of standard cell culture medium) Na^+ in 0.5, 1, 3, 6 and 24 h; 30 mM mannitol was added to the control medium for the maintaining isoosmolarity.

2.3. The atomic force microscopy (AFM) measurements of HUVEC

Experiments on living cells were carried out immediately after they were removed from the CO_2 incubator. The AFM measurements of HUVEC were performed at 37 °C using a commercial atomic force microscope Solver Bio (NT-MDT, Moscow, Russia), combined with an

inverted optical microscope Olympus IX71 (Tokyo, Japan). For force spectroscopy experiments on living cells, we used tipless AFM probes CPC (NT-MDT) modified with a 3.25 μm radius polystyrene bead. Parameters of the modified cantilever were as follows: length – 450 μm , width – 50 μm , thickness – 2 μm , and the mean force constant of 0.205 N m^{-1} .

Cover glasses with cells were placed in the Petri dish with cell culture medium. Young's moduli were measured in control culture medium, in control culture medium with additional 15 mM NaCl and in control culture medium with additional 30 mM mannitol in 30 min after addition of NaCl or mannitol and after 24 h incubation in correspondent media. Before and after measurements, the relationship between the photodiode signal and cantilever deflection was calibrated by recording several force curves at a bare region of the cover glass surface, followed by measuring the slope. To measure Young's moduli, 10 force curves were taken on each cell. Force curves were obtained and processed according to a procedure described elsewhere (Hermanowicz et al., 2014; Efremov et al., 2015; Vakhruшева et al., 2019) with AtomicJ software (<https://sourceforge.net/projects/jrobust/>). Young's moduli were calculated by interpreting the obtained force curves using the Sneddon model for a spherical surface, which is suitable for cantilevers modified by microspheres. Using a microsphere instead of a sharp needle allows for better control of the probe geometry and prevents cell damage. The average indentation depth was 200 nm.

2.4. Measurement of the equivalent elastic constant, k_e , of HUVEC's membranes

The study was carried out using an automated MIA-D interference microscope constructed at the All-Russian Research Institute of Optical and Physical Measurements and based on a MI-4 Linnik interferometer (LOMO, St. Petersburg, Russia) (Minaev and Yusipovich 2012; Levin et al. 2013). This technique provides a phase image (PI) of an object (we can quantitatively evaluate the value of phase or proportional value – optical path difference at each point of PI). Root mean squared amplitude of cell membrane thickness fluctuations, s_t , used for estimation of magnitude of living cell membrane fluctuations. The measurement procedure is described in detail in (Parshina et al., 2019). In short: (a) recording a series of PI (512 images at 25 Hz); (b) calculate a z-projection of the PI series, representing the projection of stacked images along the axis perpendicular to an image plane and containing a root mean squared amplitude fluctuation of the temporal optical path difference (OPD) oscillation of each pixel of the projection; (c) calculate of the average value of root mean squared amplitude fluctuation of temporal OPD oscillation for the entire z-projection of the cell (without values from the cell boundary); (d) calculate the average value of root mean squared amplitude fluctuation of temporal OPD oscillation, s_{cell} , only for cell without noise; and (e) calculate the value of s_t (Rappaz et al., 2009): $s_t = s_{cell}/(n - n_0)$, where n – is a refractive index of cell (about 1.404); n_0 – is a refractive index of a buffer solution (1.335) (Yusipovich et al., 2009). Then the root mean squared amplitude of cell membrane fluctuations, s_t , used to calculate k_e as follows (Popescu et al., 2006): $k_e = \frac{k_B T}{s_t^2}$, where k_B is the Boltzmann constant and T is the temperature (Kelvin degrees).

The vertical resolution was equal to 1.9 nm; the horizontal resolution was about 0.5 μm ; repeatability of measurements results was less than 0.1 nm.

Before measurements, the cover glass with attached cells was placed on a mirror surface (cells to the mirror) at 37 °C.

2.5. Measurement of intracellular Na^+ , K^+ , Rb^+

Six-well plates were transferred onto ice, experimental medium was quickly removed and cells were washed three times with 3 ml of an ice-cold 0.1 M $MgCl_2$ solution in doubly deionized (DDI) water. Then, 1.5 ml of 5% trichloroacetic acid (TCA) in DDI water were added to each well,

followed by incubation at 4 °C overnight for complete extracting of ions from cells. Cell precipitates were suspended and centrifuged during 5 min at 15000 g. Supernatants were transferred into test tubes and stored at -20 °C. Cell precipitates were resuspended in 0.75 ml of 0.1 M NaOH and incubated at 65 °C during 1 h for complete protein dissolving. The protein solutions gained were used for protein amount quantification by Lowry protein assay (Lowry et al., 1951). The Na⁺_i and K⁺_i contents in TCA extracts were measured by flame atomic absorption spectrometry using the Kvant-2m1 spectrometer (Cortec, Russia) with propane-air mixture at 589 nm and 766.5 nm, respectively. KCl (0.5–4 mg L⁻¹ K⁺) and NaCl solutions (0.05–2 mg L⁻¹ Na⁺) in 5% TCA in DDI water were used for calibration. The Rb⁺_i content was determined by the same method at 780 nm, RbCl (0.2–4 mg/L Rb⁺) in 5% TCA in DDI water was used for calibration. To study the rate of Rb⁺ influx, we added 2.5 mM RbCl to the medium 10 min before the end of incubation, since during this period the accumulation of Rb⁺ inside the cell occurs linearly. The Na⁺_i, K⁺_i and Rb⁺_i contents in each well were normalized on protein amount in the same well.

2.6. Real-time quantitative RT-PCR

HUVEC cells (~10 × 10⁴ cells) were washed with an ice-cold PBS buffer and an appropriate volume of Trizol reagent was added in order to isolate the total RNA. After isolation of the aqueous phase containing nucleic acids using chloroform and treatment with 96% ethanol, further steps of RNA isolation and treatment with DNase were performed on Quick-RNA MicroPrep microkit columns. The ImProm-ITM Reverse Transcription System kit was used for the reverse transcription reaction. In all cases, procedures were followed according to the manufacturer's instructions. The real-time PCR was carried out with Bio-Rad Real-Time PCR System (Bio-Rad, California, Hercules, CA, USA). Primers (Syntol, Moscow, Russia, Table 1) were added to a final concentration of 160 nM. Amplification modes: 95 °C 5 min; 95 °C 10 s; 58 °C 17 s; 72 °C 20 s; 40 repetitions of steps 95 °C 10 s, 58 °C 17 s, 72 °C 20 s; melting curve from 72 to 95 °C, increment 0.5 °C 5 s. The selection of primers was performed using the Beacon Designer 7 program, as well as using the NCBI and BLAT search databases. The expression level of each gene of interest was calculated using the reference GAPDH (glyceraldehyde 3-phosphate dehydrogenase) gene by the ΔΔCt method (Vandesompele et al., 2002). Gene expression in the control was taken as 100%. To verify the PCR products, they were sequenced. Electrophoresis was performed in 2% agarose gel using TBE buffer in the presence of ethidium bromide for ~1h at 75 mV. PCR products were extracted from the gel using a QIAquick Gel Extraction Kit according to the manufacturer's protocol. DNA sequencing was carried out by Genom (Moscow, Russia). The sequences were aligned using the BLAST program. All DNA sequences were as stated.

2.7. The isolation of cytoplasmic and nuclear fractions

Cells after treatment were scraped off at 37 °C and centrifuged during 5 min at 1000 g, 4 °C. Pellets were resuspended in 200 μl of cold buffer A (10 mM HEPES, pH 7.9; 1.5 mM MgCl₂; 10 mM KCl; protease inhibitor cocktail) and incubated for 15 min on ice. Then, 0.6% Nonidet P-40 was added to each sample, followed by centrifugation during 1 min at 14000 g, 4 °C. Supernatants were used as cytoplasmic fractions. Pellets were resuspended in 50 μl of RIPA buffer containing protease inhibitor cocktail and shaken vigorously. The suspension was centrifuged for 20 min at 14000 g, 4 °C, supernatants were used as nuclear fractions. Protein concentrations were determined using Lowry protein assay (Lowry et al., 1951).

2.8. Western blot analysis

Protein samples were analysed by SDS-PAGE according to the Laemmli technique (Laemmli 1970) (4% stacking gel, 10% separating

gel) and transferred onto a nitrocellulose membrane (Bio-Rad, California, Hercules, CA, USA) for 30 min in a semi-dry Trans-blot Turbo, Standard SD mode (Bio-Rad, California, Hercules, CA, USA). Following electro-transfer, the membrane was blocked with 5% Milk/TBS solution for 1 h and incubated with a rabbit polyclonal antibody recognizing NFAT5 (#PA1-023, ThermoFisher Scientific, Massachusetts, Waltham, MA, USA) at a dilution of 1:1000 overnight at 4 °C on a rocking platform and with goat anti-rabbit IgG peroxidase conjugated antibody (AP132P, Sigma Aldrich, Darmstadt, Germany) at a dilution of 1:25000 for 1 h at 37 °C. The total amount of NFAT5 was normalized to β-actin (#4970, Cell Signaling Technology, Massachusetts, Danvers, MA, USA, 1:1000). The cytosolic and nuclear NFAT5 content was normalized by incubation with primary antibodies to GAPDH (sc-32233, Santa Cruz Biotechnology, Texas, Dallas, TX, USA, 1:3000) and to lamin-B1 (sc-56145, Santa Cruz Biotechnology, Texas, Dallas, TX, USA, 1:1000) for 1 h at room temperature, respectively. The membranes were then washed by TBST and incubated with secondary peroxidase conjugated antibodies to mouse IgG (A-9044, Sigma Aldrich, Darmstadt, Germany, 1:1000) or rabbit IgG (AP132P, Sigma Aldrich, Darmstadt, Germany, 1:1000) for 1 h at room temperature. Antibodies bound to the membrane were detected using chemiluminescent SuperSignal™ West Femto Maximum Sensitivity Substrate ECL kit in an Endolab ChemiDoc XRSplus instrument (Bio-Rad, California, Hercules, CA, USA). Relative protein content was assessed using densitometry with ImageLab™ 3.0 software (Bio-Rad, California, Hercules, CA, USA).

Table 1. Primer sequences used in this study.

Gene Symbol	Human gene name, PCR product size (nucleotide pairs)	bp	GenBank mRNA sequence number	Primer nucleotide sequence
FOS	Fos proto-oncogene, AP-1 transcription factor subunit	154	NM_005252	F: 5'-GCA AGG TGG AAC AGT TAT CTC-3' R: 5'-GCA GAC TTC TCA TCT TCT AGT TG -3'
IL6	Interleukin 6	195	NM_000600.4	F: 5'-CAG ATT TGA GAG TAG TGA GGA AC-3' R: 5'-CGC AGA ATG AGA TGA GTT GTC-3'
IL1RL1	Interleukin 1 receptor like 1	247	NM_003856	F: 5'-GAA ATC GTG TGT TTG CCT CAG-3' R: 5'-GGT GCT GTC CAG TTG TAG AG-3'
NOS3	Nitric oxide synthase 3	102	NM_001160109.2	F: 5'-GCA ACC ACA TCA AGT ATG CC-3' R: 5'-TGT TCC AGA TTC GGA AGT CTC-3'
PTGS2	Prostaglandin-endoperoxide synthase 2	156	NM_000963.4	F: 5'-GTA TGT ATG AGT GTG GGA TTT GAC-3' R: 5'-CTT GAA GTG GGT AAG TAT GTA GTG-3'
GAPDH	Glyceraldehyde-3-phosphate dehydrogenase	131	NM_002046.7	F: 5'-CCT GGT ATG ACA ACG AAT TTG-3' R: 5'-CAG TGA GGG TCT CTC TCT TCC-3'

2.9. Statistical analysis

The results from microscopy methods were statistically processed using Graphpad Prism 9.0 demo software (GraphPad Software, La Jolla California, USA). D'Agostino & Pearson omnibus normality test ($p < 0.05$) used to examine the normality of data. The other statistical procedure is described in figures captions.

3. Results

3.1. Elevated extracellular NaCl triggers changes in monovalent cations fluxes

Our previous studies have demonstrated that appreciable Na^+/K^+ imbalance induced by Na,K-ATPase inhibition triggers subsequent transcriptional changes in various types of cells (Koltsova et al., 2012; Klimanova et al., 2019). In the present study human endothelial cells were incubated in the medium with moderately increased Na^+ concentration for 1, 3, 6 and 24 h with consequent measurement of Na^+ and K^+ intracellular content. Figure 1A demonstrates a small but statistically significant decrease in the intracellular Na^+ content in response to the elevation in extracellular NaCl by 15 mM for 1 h. No statistically significant alterations in the intracellular Na^+ content were observed upon this treatment for 3, 6 and 24 h. As shown in Figure 1B, the intracellular K^+ content was not statistically changed in the presence of additional 15 mM NaCl up to 24 h. Since the amount of K^+ is quite large, its small change is difficult to register. In this regard, we studied Rb^+ influx. Rb^+ as a K^+ congener is widely used to estimate transport of K^+ into cells. Since the content of Rb^+ in cells is very small, its increment is easy to detect. As we can see, an enhanced Rb^+ influx was observed with elevated-salt exposure of HUVEC for 1 and 3 h (Figure 1C).

The augmentation in Rb^+ influx may be associated with the activation of Na,K-ATPase and/or Na-K-2Cl-cotransporter by increased intracellular Na^+ , which, in turn, appears to be the result of enhanced Na^+ influx due to its increase in the extracellular medium. Amiloride-sensitive Na^+ channels have been shown to facilitate the inward Na^+ current in endothelial cells (Wang et al., 2009). We did not observe any changes in Na^+ , K^+ content and Rb^+ influx in response to an increase in

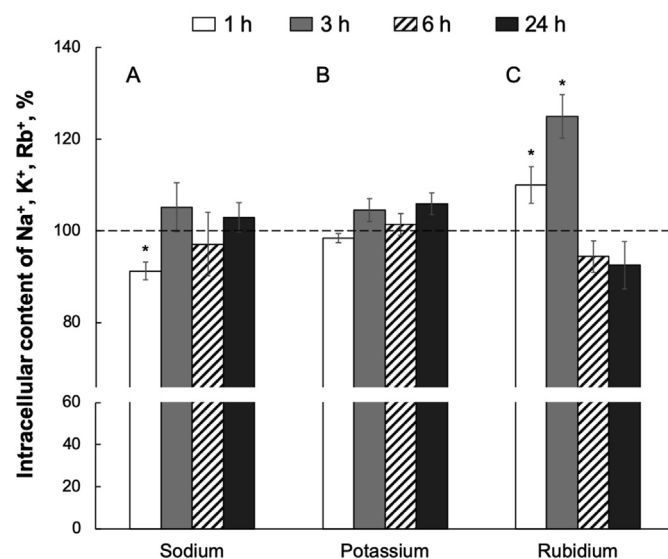


Figure 1. Time-dependent action of elevated extracellular NaCl on Na^+ (A), K^+ (B) content and Rb^+ influx (C) in HUVEC. Cells were subjected to control cell culture medium containing additional 15 mM NaCl for 1, 3, 6 and 24 h. Baseline values of K^+ , Na^+ and Rb^+ content obtained in the control for each time point were taken as 100%. The significant differences were calculated using the rank-based nonparametric Kruskal-Wallis ANOVA test. * - $p < 0.05$ compared to control cells. Means \pm S.E. are shown, $n = 6-12$.

extracellular NaCl in the presence of 1 μM amiloride either for 1 h (Figure 2A-C) or 3 h (Figure 2D-F) of incubation. These data demonstrate that amiloride-sensitive Na^+ channels are involved in the changes in monovalent cation fluxes that we observed in response to an elevation of extracellular NaCl concentration (Figure 1). Barbaro and colleagues have previously shown that sodium entry into high-salt-treated dendritic cells is also mediated by amiloride-sensitive Na^+ channels (Barbaro et al., 2017).

Enhanced Na^+ influx leads to an increase in its intracellular content. Na,K-ATPase-activating effect of Na^+ ions has been previously described (Skou and Esmann 1992; Therien et al., 1996). Indeed, in the presence of 3 μM ouabain, we observed an increase in intracellular Na^+ content in HUVEC upon their exposure to the medium with an elevated NaCl concentration for 1–3 h (Figure 3A, D). However, the change in this parameter after 1 h of incubation was not significant (Figure 3A). Intracellular K^+ content was decreased after 1 and 3 h of Na,K-ATPase inhibition (Figure 3B, E), but an even greater decrease was observed after 3 h of incubation in a medium with additional 15 mM NaCl in the presence of 3 μM ouabain (Figure 3E). However, no differences in Rb^+ influx were detected (Figure 3C, F). Summarizing these data, we can conclude that, in response to an elevation in NaCl concentration in the medium, endothelial cells tend to support gradient of monovalent cations by the activation of Na,K-ATPase. Moreover, the activation of Na, K-ATPase in endothelial cells by elevated extracellular NaCl has been demonstrated earlier (Korte et al., 2012).

Therefore, cells appear to maintain sodium homeostasis in response to the increase in extracellular Na^+ . It should be noted that the change in osmolarity induced by the addition of 30 mM mannitol did not affect intracellular content of monovalent cations in endothelial cells (Figure 4). It demonstrates that the alteration in the monovalent cations fluxes across the plasma membrane depends more on NaCl concentration than on osmolarity of the extracellular medium.

3.2. Na^+/K^+ perturbations affect gene expression

We investigated whether moderate augmentation in extracellular NaCl (additional 15 mM) influences gene expression. Tested genes (*NOS3* (nitric oxide synthase 3)), *FOS* (Fos proto-oncogene), *PTGS2* (prostaglandin-endoperoxide synthase 2), *IL6* (interleukin 6), *IL1LR1* (interleukin 1 receptor like 1)) were chosen for the study because of their well-documented importance in endothelium functioning and involvement in the proinflammatory response (Moncada and Higgs 2006; DebRoy et al., 2014; Muñoz and Ana, 2015; Rincon 2012; Choi et al., 2009). In addition, it was reported that dissipation of the Na^+/K^+ gradient in HeLa (human malignant epithelial cells), HUVEC and RVMSC (rat vascular smooth muscle cells) affects *FOS*, *IL6*, *PTGS2* transcription via Ca^{2+} -independent mechanism(s) (Koltsova et al., 2012). Figure 5 displays that exposure of HUVEC to the medium with elevated NaCl decreased the content of mRNAs encoding *PTGS2* after 3, 6 and 24 h of incubation. *IL1LR1* gene was downregulated at increased-salt stimulation for 6 and 24 h. The content of *IL6* gene mRNAs was significantly decreased all the time. The expression of *FOS* and *NOS3* genes remained statistically unchanged in the presence of additional 15 mM NaCl. We may conclude that alterations in the transcription of above-listed genes are due to exactly Na^+/K^+ perturbations because the change in osmolarity of the extracellular medium induced by the addition of mannitol didn't affect either monovalent cations intracellular content (Figure 4) or tested genes expression (Figure 6). Weik and co-workers have previously demonstrated that compatible organic osmolytes diminished *PTGS2* expression triggered by the hyperosmotic effect of lipopolysaccharide-stimulated rat liver sinusoidal endothelial cells (Weik et al., 1998). Most likely, the accumulation of these substances led to the alterations in Na^+/K^+ activities and a subsequent decrease in *PTGS2* mRNA levels.

As noted above, one potential mechanism of gene expression alterations in endothelial cells in response to the osmolarity change can be NFAT5-dependent regulation of transcription (Dmitrieva and Burg

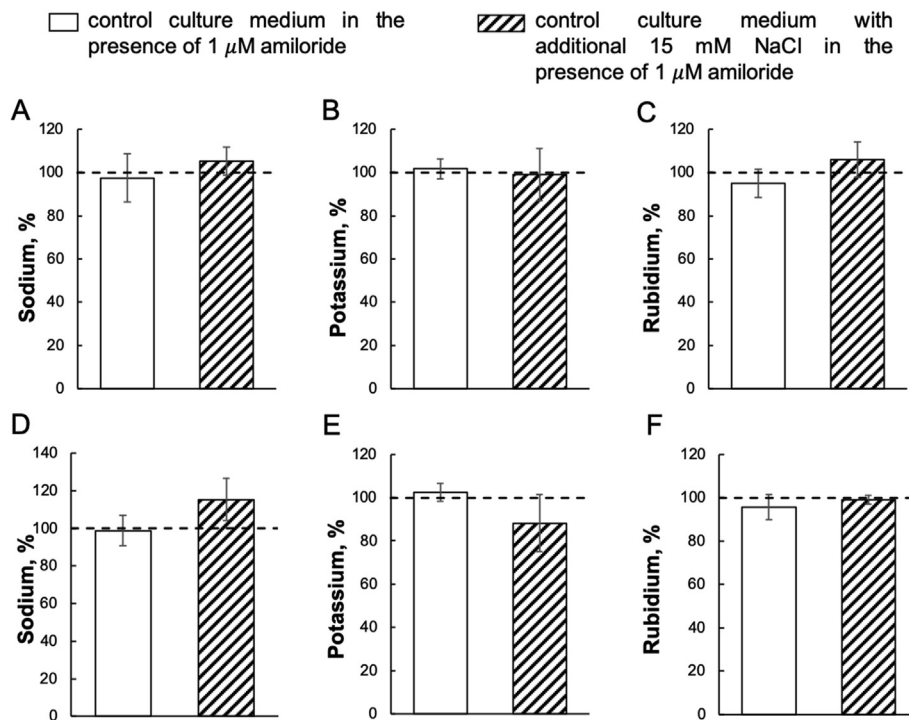


Figure 2. Effect of 1 μM amiloride on the content of Na⁺_i and K⁺_i, and Rb⁺ influx in HUVEC. Cells were incubated in control culture medium and in culture medium with additional 15 mM NaCl for 1 (A, B, C) and 3 (D, E, F) hours. To study the rate of Rb⁺ influx, we added 2.5 mM RbCl to the medium 10 min before the end of incubation. K⁺_i, Na⁺_i and Rb⁺_i content in cells for each time point in the absence of amiloride was taken as 100%. The significant differences were calculated using the One-way ANOVA test. Means ± S.E. are shown, n = 4–14.

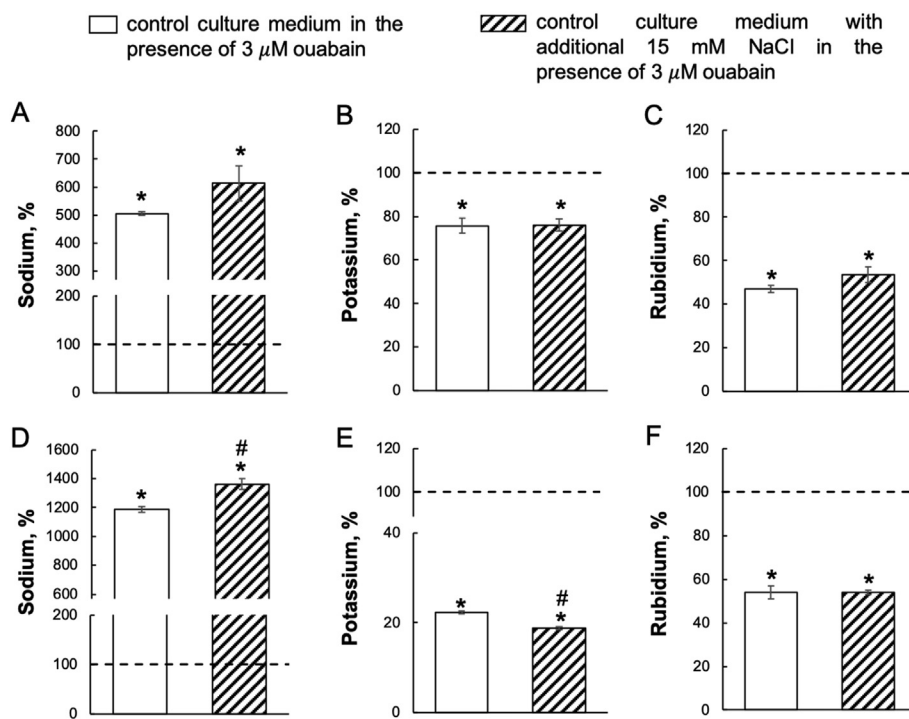


Figure 3. Effect of 3 μM ouabain on the content of Na⁺_i and K⁺_i, and Rb⁺ influx in HUVEC. Cells were incubated in control culture medium and in culture medium with additional 15 mM NaCl for 1 (A, B, C) and 3 (D, E, F) hours. To study the rate of Rb⁺ influx, we added 2.5 mM RbCl to the medium 10 min before the end of incubation. K⁺_i, Na⁺_i and Rb⁺_i content in cells for each time point in the absence of ouabain was taken as 100%. The significant differences were calculated using the One-way ANOVA test. * - p < 0.05 compared to control cells; # - p < 0.05 compared to cells incubated in culture medium in the presence of ouabain. Means ± S.E. are shown, n = 4–14.

2014). In addition, it was shown that NFAT5 expression can not only be increased, but also be suppressed depending on the cellular ionic strength (Woo et al., 2000). However, we did not detect an altered abundance of NFAT5 protein in response to the elevation of extracellular NaCl by 15 mM within 24 h (Figure 7). Taking into account the fact that NFAT5 is a nuclear transcription factor, we determined its nuclear and cytosolic distribution. As shown in Figure 8, an overwhelming amount of this transcription factor was detected in the nuclear fractions of cells. It is important to note that no significant differences were found in the content of nuclear NFAT5 in cells treated with excess NaCl or mannitol for 1,

3, 6, and 24 h. These findings support the idea that Na⁺_i/K⁺_i-dependent mechanism of transcription regulation takes place. The molecular origin of Na⁺_i/K⁺_i sensor(s) involved in this process should be identified in forthcoming studies.

3.2. Moderate hyperosmotic stimulation of HUVEC for 24 h didn't affect cellular mechanical properties

The term “cell stiffness”, or rigidity, although commonly has no unambiguous definition in physics as a term. Usually the stiffness is

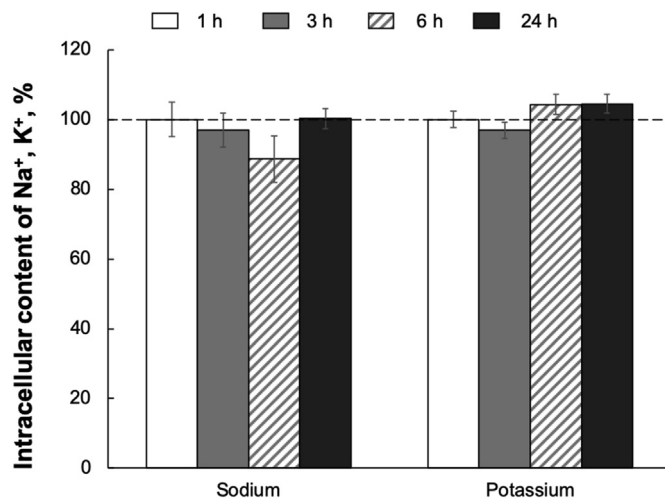


Figure 4. Time-dependent effect of 30 mM mannitol on Na^+ and K^+ content in HUVEC. Mannitol was added to the control medium for the maintaining iso-osmolality. Baseline values obtained in the control were taken as 100%. Means \pm S.E. are shown, $n = 6-12$.

understood as a measure of the resistance of a material to deformation as mechanical forces are applied to it (Janmey et al. 2019). The stiffness can depend on the geometry, time, degree of deformation, state of cell compartments, especially membrane and cytoskeleton, adhesion, etc. Atomic force microscopy (AFM) is one of the most popular method used to evaluate cell stiffness. Using AFM, it is possible to estimate Young's modulus (elasticity modulus). This value depends on cytoskeleton condition. Moreover, living cells are characterized by local membrane fluctuations or flickering (low-frequency vibrating movements about 100 nm scale amplitudes at frequencies 0.1–30 Hz) (Brochard and Lennon 1975). In this case, the term “membrane” is usually used as an acronym of the term “membrane–cytoskeleton complex”. The fluctuation depends on lateral tension (inversely), cell adhesion and other mechanical characteristics (Kononenko 2009). Moreover, membrane fluctuations can be driven by force generating processes such as ion pumps or lipid transporters activity or *via* mechanical coupling to the underlying cytoskeleton (Turlier and Betz 2018). Using membrane fluctuations, we can calculate the equivalent elastic constant of cell membranes, k_e , which depends on the bending modulus, lateral surface tension (Popescu et al.,

2006) and, to a lesser extent, other parameters. Under normal conditions, surface tension usually makes the main contribution to k_e .

Endothelial flexibility is a necessary factor for its normal function (Lang 2011). In accordance with previous publications, even a small increase in extracellular Na^+ leads to increased stiffness of the vascular endothelium and affects its functional properties (H. E. de Wardener et al., 2007). We studied the effect of additional extracellular Na^+ (+15 mM) on the endothelial cell stiffness using the force curve method and assessment of plasma membrane fluctuations. These approaches allow to determine Young's moduli (elasticity moduli) and equivalent elastic constants of membranes, respectively, which reflect the degree of cell stiffness. Measurements were performed after 0.5 and 24 h of cells exposure to the medium with excess Na^+ . To control the effect of extracellular osmolality, we used the addition of 30 mM mannitol instead of 15 mM NaCl. In our experimental conditions, we detected an increase in Young's modulus (Figure 9) and a decrease in equivalent elastic constants (Figure 10). However, compared to control samples (normal Na^+), we found that the change in these parameters developed over time and did not depend on the osmolality of the extracellular medium (Figures 9 and 10). Sodium effect on endothelial stiffness has been demonstrated earlier to be dependent on aldosterone (H. E. de Wardener et al., 2007). However, moderate elevation of extracellular Na^+ (+15 mM) also didn't affect endothelial cell stiffening in the presence of 1 nM aldosterone up to 48 h in our experiments (data not shown). On the other hand, it was shown that a pronounced effect of Na^+ on the mechanical properties of the endothelium is observed at its concentration above 139 mM (Hans Oberleithner, Kusche-Vihrog, and Schillers 2010). Summarizing these results, we can speculate that cell stiffening mediated by extracellular Na^+ depends on its concentration.

4. Discussion

In this study, we examined the effects of short-term exposure of HUVEC to moderately elevated sodium (within the physiological range) on gene expression and cellular mechanical properties. These parameters are believed to be physiological mediators that induce endothelial dysfunction.

We found that elevated extracellular sodium downregulates expression of some genes related to the inflammatory response (*PTGS2*, *IL6*, *IL1LR1*). Our results strongly suggest that Na^+/K^+ alterations play a key role in affecting the transcription of these genes in endothelial cells exposed to hyperosmotic conditions. This conclusion is supported by evidences listed below.

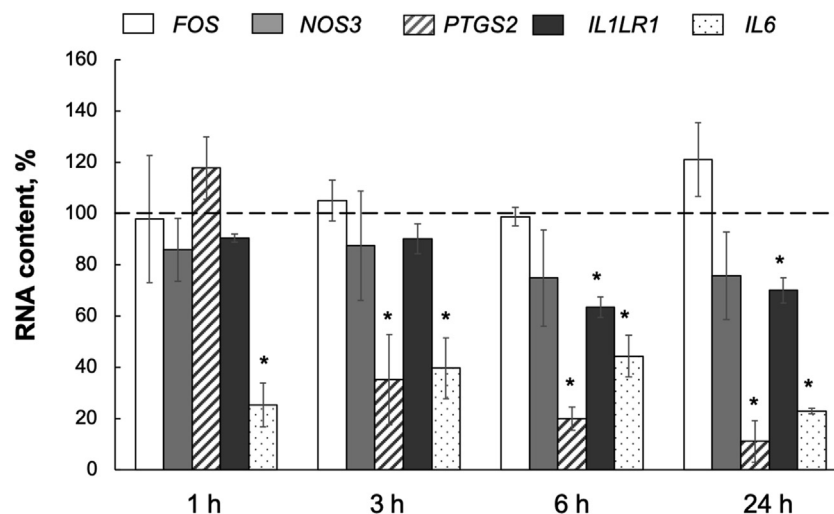


Figure 5. Time-dependent action of elevated extracellular NaCl on gene transcription in HUVEC. Cells were subjected to control cell culture medium containing additional 15 mM NaCl for 1, 3, 6 and 24 h mRNA content in control cells is taken as 100%. The significant differences were calculated using the One-way ANOVA test. * - $p < 0.05$ compared to control cells. Means \pm S.E. from 3 experiments performed in triplicate are shown.

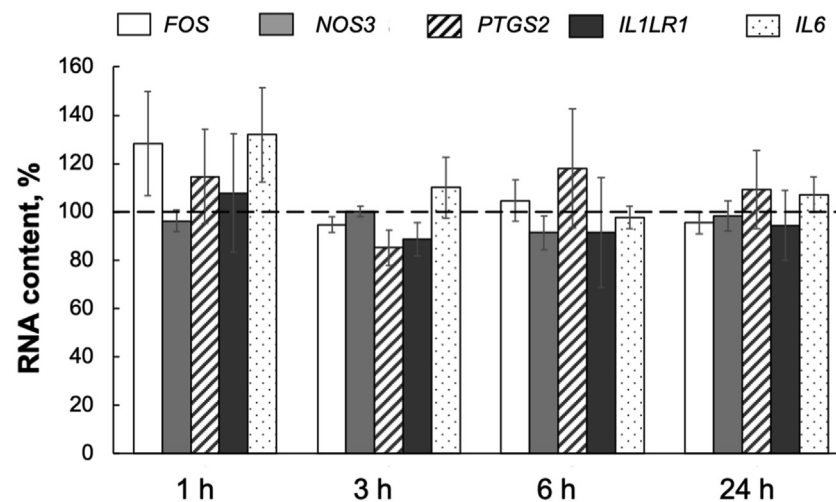


Figure 6. Effect of 30 mM mannitol on gene transcription in HUVEC. Cells were subjected to control cell culture medium containing additional 30 mM mannitol for 1, 3, 6 and 24 h mRNA content in control cells is taken as 100%. Means \pm S.E. from 3 experiments performed in triplicate are shown.

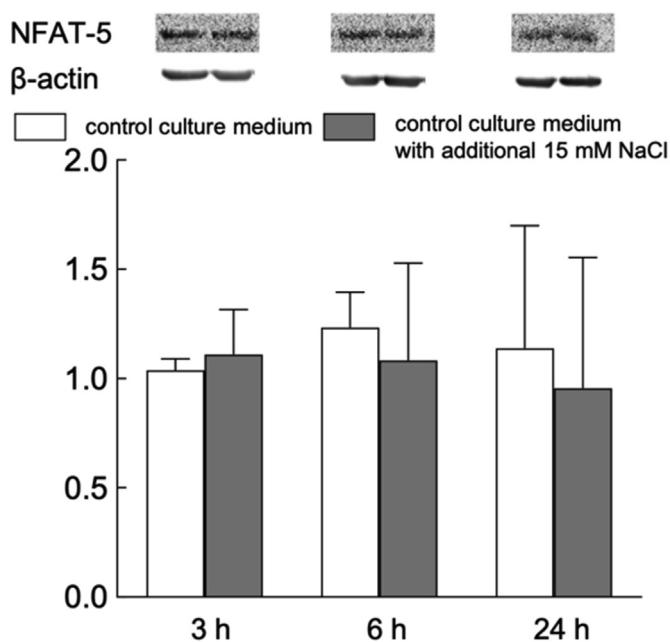


Figure 7. Representative Western blots and relative content of NFAT5 in HUVEC exposed to normal- and elevated-sodium medium for 3, 6 and 24 h. The content of proteins in control cells was taken as 1.0. Data obtained in three independent experiments are reported as means \pm S.E.

First, an increase in extracellular $[Na^+]_o$ from 125 to 140 mM influenced the Na^+_i/K^+_i gradient in HUVEC. Second, *PTGS2*, *IL6*, *IL1LR1* were found to be downregulated upon cells exposure to elevated sodium. Third, we did not detect an altered abundance of cytosolic and nuclear NFAT5 protein in response to the increase in extracellular sodium by 15 mM within 24 h. Fourth, neither Na^+_i/K^+_i ratio, nor the content of *PTGS2*, *IL6*, *IL1LR1* was affected by exposure of HUVEC to the control medium containing additional 30 mM mannitol. Fifth, the change in osmolarity of the extracellular medium, either due to the addition of NaCl or mannitol, had no effect on the mechanical properties of endothelial cells.

We should take into account that Na^+_i/K^+_i imbalance in HUVEC observed in our experiments may result in slight $[Ca^{2+}]_i$ alterations (e.g., through Na^+/Ca^{2+} exchanger), which, in turn, lead to gene expression changes. However, to assess the role of this mechanism is necessary to determine how $[Ca^{2+}]_i$ in endothelial cells varies in response to an

increase in the extracellular sodium. At the same time, it has been shown that prominent transcriptomic changes in various types of cells in the presence of extracellular Ca^{2+} -chelators are at least partially mediated by an elevation of the $[Na^+]_i/[K^+]_i$ ratio and activation of Ca^{2+} -independent, $[Na^+]_i/[K^+]_i$ -mediated mechanism of excitation-transcription coupling (Koltsova et al., 2012). All these data demonstrate that moderate and short-term elevation of extracellular sodium can affect endothelial function regardless of alterations in its mechanical parameters. This effect may be mediated by Na^+_i/K^+_i -sensitive mechanism(s) of gene transcription regulation and is not associated with changes in the osmolarity of extracellular fluids.

At first glance, the results demonstrating downregulation of the proinflammatory genes in response to an elevation of the extracellular sodium concentration seem paradoxical. Indeed, contrary to previously observed data, we detect not an increase, but a decrease in the inflammatory response under these conditions. However, there is a correlation between the change in the intracellular Na^+ content and the induction of a pro- or anti-inflammatory response. Short-term stimulation of endothelial cells with moderately increased sodium in the physiological range leads to a decrease in the intracellular Na^+ content as a result of Na,K -ATPase activation that, in turn, maintains Na^+ homeostasis in the cell. Apparently, a decrease in the intracellular Na^+ content causes an anti-inflammatory effect, and its increase as a result of Na,K -ATPase inhibition triggers pro-inflammatory genes upregulation, as we have shown earlier (Klimanova et al. 2017, 2020).

Unfortunately, not all studies have investigated how the intracellular monovalent cations content alters in response to an elevation in the extracellular Na^+ concentration. Nevertheless, an analysis of those studies in which these data were presented shows that a change in the osmolarity of the extracellular medium, which is not accompanied by an Na^+_i/K^+_i imbalance (for example, using nonpermeant osmolytes), does not trigger prominent transcriptomic changes. These changes, according to our observations, are the result of the Na^+_i/K^+_i perturbation itself. This suggestion is consistent with the observations of other researchers. Thus, it was shown that an increase in the extracellular Na^+ concentration triggers its augmented input into epithelial cells by Na_x channel and the subsequent upregulation of proinflammatory genes. At the same time, Na_x downregulation led to a decrease in the expression of these genes, including *PTGS2*, and prevented Na^+ accumulation in the cell (Xu et al., 2015; Hou et al., 2021). In another study, it was demonstrated that high-salt diet leads to the accumulation of Na^+ ions in tumor tissues and inhibits their growth in mice. Gene expression analysis of myeloid-derived suppressor cells isolated from these tumor tissues revealed that these cells have a pro-inflammatory phenotype as a result of

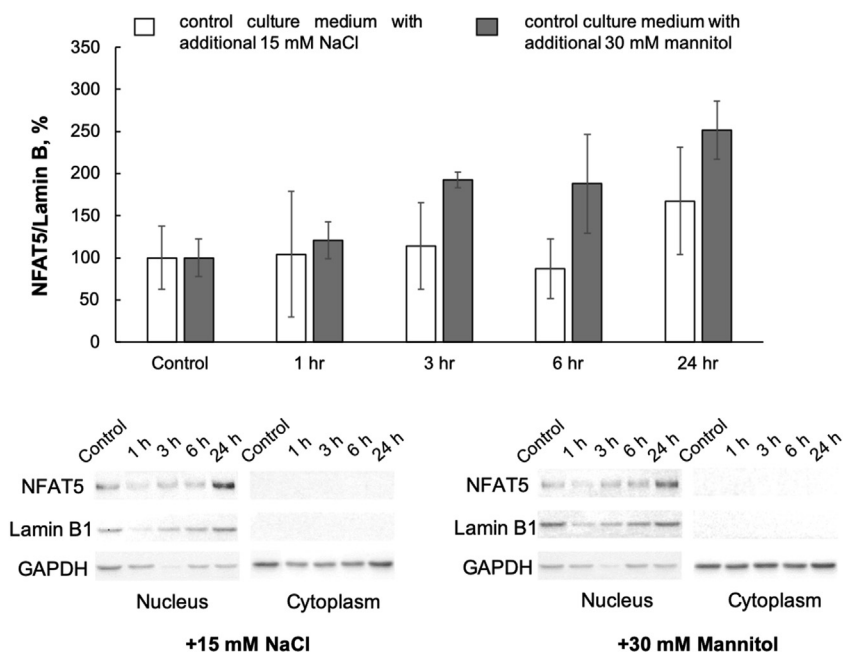


Figure 8. Representative Western blots and relative cytosol and nuclear content of NFAT5 and Lamin B1 in HUVEC exposed to normal- and elevated-sodium medium for 1, 3, 6 and 24 h. The content of proteins in control cells was taken as 1.0. Data obtained in three independent experiments are reported as means \pm S.E.

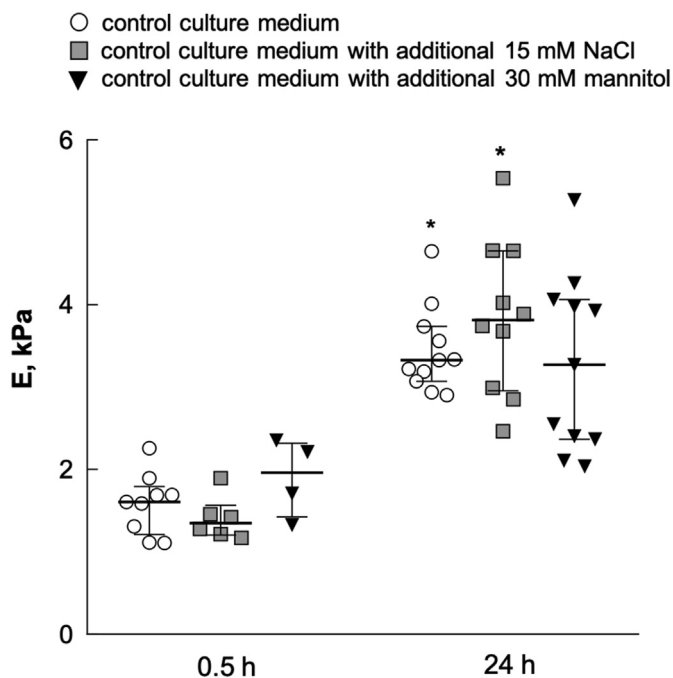


Figure 9. Effect of osmolarity of the cell culture medium on Young's modulus of HUVEC. The data shown as experimental values (points) and median with interquartile range (black lines). The significant differences were calculated using the Kruskal-Wallis test, $p < 0.05$. The significant differences between cells incubated in different media for 0.5 and 24 h, correspondingly, were not observed. * - $p < 0.05$ compared to control cells incubated for 0.5 h.

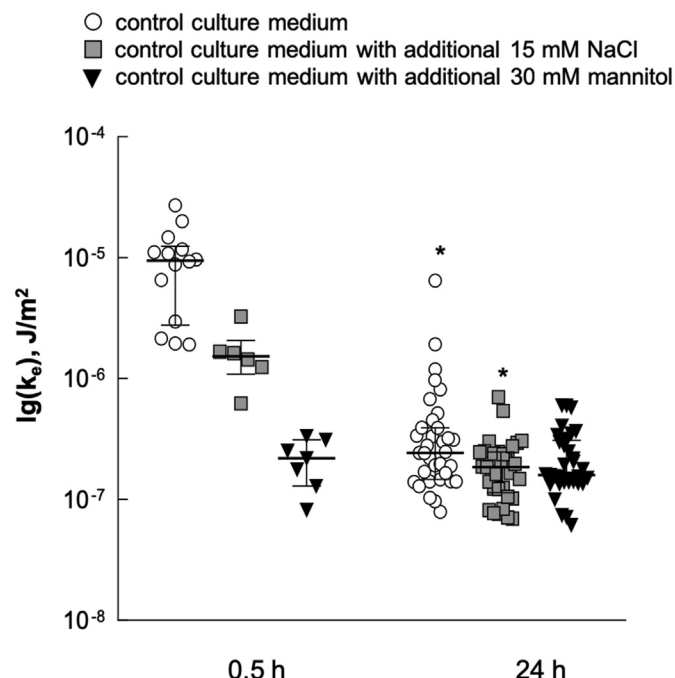


Figure 10. Effect of osmolarity of the cell culture medium on equivalent elastic constants of HUVEC. The data shown as experimental values (points) and median with interquartile range (black lines). The significant differences were calculated using the Kruskal-Wallis test, $p < 0.05$. The significant differences between cells incubated in different solutions for 0.5 and 24 h, correspondingly, were not observed. * - $p < 0.05$ compared to control cells incubated for 0.5 h.

prominent transcriptomic changes in comparison with cells of normal-salt-diet animals (He et al., 2020). Barbaro and colleagues in experiments with dendritic cells showed that these cells, in response to high-salt-treatment (but not mannitol), increase the production of the pro-inflammatory interleukin $\text{IL-1}\beta$. Nevertheless, it should keep in mind that an increase in the intracellular Na^+ content in response to an

increase in the concentration of this ion in the medium was accompanied by the activation of Ca^{2+} -dependent signaling pathways. It is useful to note that these experiments were carried out in the presence of 190 mM NaCl for 24 h, which can activate Ca^{2+} -signaling and further affect gene expression (Barbaro et al., 2017).

It is well known that NFAT5 plays a key role in the adaptation of cells to conditions of increased Na^+ content in the extracellular medium (Cheung and Ko 2013). In our experiments, we did not detect abundance alterations of this transcription factor, which would indicate its contribution to the regulation of the expression of the studied genes. Nevertheless, Neubert and colleagues showed that high-salt treatment (but not mannitol) of *E. coli*-infected mice macrophages was accompanied by rapid Na^+ influx and subsequent increased *Nfat5* expression and triggered transcriptomic changes in infected cells. However, some genes whose expression affected under high-salt conditions were not influenced by *Nfat5*-silencing (Neubert et al., 2019). All these data together clearly demonstrate that the extracellular sodium itself (the Na^+/K^+ imbalance, as consequence), but not the hyperosmotic stimulation and/or cell stiffening, can independently regulate gene expression in endothelial cells.

The next question that should be addressed is the nature of monovalent cations intracellular sensor(s). From our point of view, G-quadruplexes located within the DNA are the most suitable candidate for this role. These secondary structures are formed within guanine-rich regions of nucleic acids and are abundant in the human genome. It was also shown that their structure is stabilized by monovalent cations in the following sequence: $\text{K}^+ > \text{Na}^+, \text{NH}_4^+ \gg \text{Li}^+$ (Kharel et al., 2020). Sen and Gilbert were the first to show that the ratio of Na^+ and K^+ ions is critical for the DNA G-quadruplexes' formation, the so-called "sodium-potassium switch" (Sen and Gilbert 1990). Moore and Morrill proposed a model according to which Na,K-ATPase activity determines the ionic composition of the nucleus and thus "play an important role in the regulation of gene activity" (Moore and Morrill 1976). Taking this into consideration, we speculate that Na^+/K^+ imbalance mediates transcriptomic changes directly, through a change in DNA conformation within G-quadruplexes. However, these assumptions require further experimental verification.

Declarations

Author contribution statement

Fedorov D.A., Yusipovich A.I., Parshina E.Y.: Conceived and designed the experiments; Performed the experiments; Analyzed and interpreted the data; Contributed reagents, materials, analysis tools or data.

Sidorenko S.V.: Analyzed and interpreted the data; Contributed reagents, materials, analysis tools or data.

Tverskoi A.M.: Performed the experiments; Contributed reagents, materials, analysis tools or data.

Abramicheva P.A.: Performed the experiments.

Maksimov G.V., Lopina O.D.: Conceived and designed the experiments; Wrote the paper.

Orlov S.N.: Conceived and designed the experiments.

Klimanova E.A.: Conceived and designed the experiments; Analyzed and interpreted the data; Contributed reagents, materials, analysis tools or data; Wrote the paper.

Funding statement

This work was supported by Russian Science Foundation, grant number 19-75-10009.

Data availability statement

Data will be made available on request.

Declaration of interests statement

The authors declare no conflict of interest.

Additional information

No additional information is available for this paper.

Acknowledgements

This research has been supported by the Interdisciplinary Scientific and Educational School of Moscow University « Molecular Technologies of the Living Systems and Synthetic Biology». Experiments were carried out using the Shared Use Equipment Centre for high-precision measuring in photonics (ckp.vniiofi.ru. VNIIOFI). The authors are grateful for the valuable help from Bukach O.V. in obtaining experimental data.

References

- Aramburu, Jose, López-Rodríguez, Cristina, 2019. Regulation of inflammatory functions of macrophages and T lymphocytes by NFAT5. *Front. Immunol.* 10, 535.
- Barbaro, Natalia R., Foss, Jason D., Kryshtal, Dmytro O., Tsyba, Nikita, Kumaresan, Shivani, Xiao, Liang, Mernaugh, Raymond L., et al., 2017. Dendritic cell amiloride-sensitive channels mediate sodium-induced inflammation and hypertension. *Cell Rep.* 21 (4), 1009–1020.
- Brochard, F., Lennon, J.F., 1975. Frequency spectrum of the flicker phenomenon in erythrocytes. *J. Phys.* 36 (11), 1035–1047.
- Charbonnier, Frank W., Zamani, Maedeh, Huang, Ngan F., 2019. Endothelial cell mechanotransduction in the dynamic vascular environment. *Adv. Biosyst.* 3 (2), 1800252.
- Cheung, Chris YK., Ko, Ben CB., 2013. "NFAT5 in cellular adaptation to hypertonic stress – regulations and functional significance. *J. Mol. Signal.* 8 (1), 5.
- Choi, Yeon-Sook, Choi, Hyun-Jung, Min, Jeong-Ki, Pyun, Bo-Jeong, Maeng, Yong-Sun, Park, Hongryeol, Kim, Jihye, Kim, Young-Myeong, Kwon, Young-Guen, 2009. Interleukin-33 induces angiogenesis and vascular permeability through ST2/TRAF6-mediated endothelial nitric oxide production. *Blood* 114 (14), 3117–3126.
- DebRoy, Auditi, Vogel, Stephen M., Soni, Dheeraj, Sundivakkam, Premanand C., Malik, Asrar B., Tirupathi, Chinnaswamy, 2014. Cooperative signaling via transcription factors NF-KB and AP1/c-Fos mediates endothelial cell STIM1 expression and hyperpermeability in response to endotoxin. *J. Biol. Chem.* 289 (35), 24188–24201.
- Dickinson, Kacie M., Clifton, Peter M., Keogh, Jennifer B., 2011. "Endothelial function is impaired after a high-salt meal in healthy subjects1–3. *Am. J. Clin. Nutr.* 93 (3), 500–505.
- Dmitrieva, Natalia I., Burg, Maurice B., 2014. Secretion of von Willebrand factor by endothelial cells links sodium to hypercoagulability and thrombosis. *Proc. Natl. Acad. Sci. Unit. States Am.* 111 (17), 6485–6490.
- Dmitrieva, Natalia I., Burg, Maurice B., 2015. Elevated sodium and dehydration stimulate inflammatory signaling in endothelial cells and promote atherosclerosis. *PLoS One* 10 (6), e0128870.
- Efremov, Yu.M., Bagrov, D.V., Kirpichnikov, M.P., Shaitan, K.V., 2015. "Application of the Johnson-Kendall-roberts model in AFM-based mechanical measurements on cells and gel. *Colloids Surf. B Biointerfaces* 134 (October), 131–139.
- Engberink, Olde, Rik, H.G., Rorije, Nienke M.G., van den Born, Bert-Jan H., Vogt, Liffert, 2017. Quantification of nonosmotic sodium storage capacity following acute hypertonic saline infusion in healthy individuals. *Kidney Int.* 91 (3), 738–745.
- Fels, Johannes, Jeggle, Pia, Liashkovich, Ivan, Peters, Wladimir, Oberleithner, Hans, 2014. Nanomechanics of vascular endothelium. *Cell Tissue Res.* 355 (3), 727–737.
- He, Wei, Xu, Jinzhi, Mu, Ruoyu, Qiu, Li, Lv, Da-lun, Huang, Zhen, Zhang, Junfeng, Wang, Chunming, Dong, Lei, 2020. High-salt diet inhibits tumour growth in mice via regulating myeloid-derived suppressor cell differentiation. *Nat. Commun.* 11 (1), 1732.
- Hermanowicz, Pawel, Sarna, Michał, Burda, Kvetoslava, Gabryś, Halina, 2014. AtomicJ: an open source software for analysis of force curves. *Rev. Sci. Instrum.* 85 (6), 063703.
- Hou, Chun, Dolivo, David, Rodrigues, Adrian, Li, Yingxing, Leung, Kai, Galiano, Robert, Seok Jong Hong, Mustoe, Thomas, 2021. Knockout of sodium channel *Na_v* delays Re-epithelialization of splinted murine excisional wounds. *Wound Repair Regen.* 29 (2), 306–315.
- Janmey, Paul A., Fletcher, Daniel A., Reinhart-King, Cynthia A., 2019. Stiffness sensing by cells. *Physiol. Rev.* 100 (2), 695–724.
- Kharel, Prakash, Balaratnam, Sumirtha, Nathan, Beals, Basu, Soumitra, 2020. The role of RNA G-quadruplexes in human diseases and therapeutic strategies. *WIREs RNA* 11 (1), e1568.
- Klimanova, Elizaveta A., Tverskoi, Artem M., Koltsova, Svetlana V., Sidorenko, Svetlana V., Lopina, Olga D., Tremblay, Johanne, Hamet, Pavel, Kapilevich, Leonid V., Orlov, Sergei N., 2017. Time- and dose dependent actions of cardiotonic steroids on transcriptome and intracellular content of Na^+ and K^+ : a comparative analysis. *Sci. Rep.* 7, 45403.
- Klimanova, Elizaveta A., Sidorenko, Svetlana V., Smolyaninova, Larisa V., Kapilevich, Leonid V., Gusakova, Svetlana V., Lopina, Olga D., Orlov, Sergei N., 2019. Ubiquitous and cell type-specific transcriptomic changes triggered by dissipation of monovalent cation gradients in rodent cells: physiological and pathophysiological implications. In: *Current Topics in Membranes*. Academic Press.
- Klimanova, Elizaveta A., Sidorenko, Svetlana V., Abramicheva, Polina A., Tverskoi, Artem M., Orlov, Sergei N., Lopina, Olga D., 2020. Transcriptomic changes in endothelial

- cells triggered by Na,K-ATPase inhibition: a search for upstream Na⁺/K⁺ sensitive genes. *Int. J. Mol. Sci.* 21 (21), 7992.
- Koltsova, Svetlana V., Trushina, Yulia, Haloui, Mounisif, Akimova, Olga A., Tremblay, Johanne, Hamet, Pavel, Orlov, Sergei N., 2012. "Ubiquitous [Na⁺]_i/[K⁺]_i Sensitive transcriptome in mammalian cells: evidence for Ca²⁺-independent excitation-transcription coupling." edited by Yoshiaki tsuji. *PLoS One* 7 (5) e38032–e38032.
- Kononenko, V.L., 2009. Flicker in erythrocytes. II. Results of experimental studies. *Biochem. Suppl. Ser. A: Membr. Cell Biol.* 3 (4), 372–387.
- Korte, Stefanie, Wiesinger, Anne, Straeter, Alexandra S., Peters, Wladimir, Oberleithner, Hans, Kusche-Vihrog, Kristina, 2012. Firewall function of the endothelial glycocalyx in the regulation of sodium homeostasis. *Pflug. Arch. Eur. J. Physiol.* 463 (2), 269–278.
- Laemmli, U.K., 1970. Cleavage of structural proteins during the assembly of the head of bacteriophage T4. *Nature* 227 (5259), 680–685.
- Lang, Florian, 2011. Stiff endothelial cell syndrome in vascular inflammation and mineralocorticoid excess. *Hypertension* 57 (2), 146–147.
- Levin, G.G., Vishnyakov, G.N., Minaev, V.L., 2013. An automated interference microscope for measuring dynamic objects. *Instrum. Exp. Tech.* 56 (6), 686–690.
- Lowry, O.H., Rosebrough, N.J., Lewis Farr, A., Randall, R.J., 1951. Protein measurement with the folin phenol reagent. *J. Biol. Chem.* 193 (1), 265–275.
- Minaev, V.L., Yusipovich, A.I., 2012. Use of an automated interference microscope in biological research. *Meas. Tech.* 55 (7), 839–844.
- Minegishi, Shintaro, Luft, Friedrich C., Titze, Jens, Kitada, Kento, 2020. Sodium handling and interaction in numerous organs. *Am. J. Hypertens.* 33 (8), 687–694.
- Moncada, S., Higgs, E.A., 2006. Nitric oxide and the vascular endothelium. In: Moncada, Salvador, Higgs, Annie (Eds.), *The Vascular Endothelium I*. Springer Berlin Heidelberg, Berlin, Heidelberg, pp. 213–254. *Handbook of Experimental Pharmacology*.
- Moore, Richard, Morrill, Gene, 1976. A possible mechanism for concentrating sodium and potassium in the cell nucleus. *Biophys. J.* 16 (5), 527–533.
- Muñoz, Mercedes, Ana, Sánchez, Martínez, María Pilar, Benedito, Sara, López-Oliva, María-Elvira, Albino, García-Sacristán, Hernández, Medardo, Prieto, Dolores, 2015. COX-2 is involved in vascular oxidative stress and endothelial dysfunction of renal interlobar arteries from obese Zucker rats. *Free Radic. Biol. Med.* 84 (July), 77–90.
- Neubert, Patrick, Weichselbaum, Andrea, Reitinger, Carmen, Schatz, Valentin, Schröder, Agnes, Ferdinand, John R., Simon, Michaela, et al., 2019. HIF1A and NFAT5 coordinate Na⁺-Boosted antibacterial defense via enhanced autophagy and autolysosomal targeting. *Autophagy* 15 (11), 1899–1916.
- Oberleithner, Hans, Wilhelm, Marianne, 2015. Vascular glycocalyx sodium store - determinant of salt sensitivity? *Blood Purif.* 39 (1–3), 7–10.
- Oberleithner, H., Callies, C., Kusche-Vihrog, K., Schillers, H., Shahin, V., Riethmüller, C., MacGregor, G.A., de Wardener, H.E., 2009. Potassium softens vascular endothelium and increases nitric oxide release. *Proc. Natl. Acad. Sci. Unit. States Am.* 106 (8), 2829–2834.
- Oberleithner, Hans, Kusche-Vihrog, Kristina, Schillers, Hermann, 2010. Endothelial cells as vascular salt sensors. *Kidney Int.* 77 (6), 490–494.
- Oh, Young S., Appel, Lawrence J., Galis, Zorina S., Hafner, David A., Jiang, He, Hernandez, Amanda L., Joe, Bina, et al., 2016. National heart, lung, and blood Institute working group report on salt in human health and sickness: building on the current scientific evidence. *Hypertension (Dallas)* 68 (2), 281–288.
- Parshina, E. Yu., Yusipovich, A.I., Brazhe, A.R., Silicheva, M.A., Maksimov, G.V., 2019. Heat damage of cytoskeleton in erythrocytes increases membrane roughness and cell rigidity. *J. Biol. Phys.* 45 (4), 367–377.
- Popescu, Gabriel, Ikeda, Takahiro, Goda, Keisuke, Catherine, A., Best-Popescu, Laposata, Michael, Manley, Suliana, Dasari, Ramachandra R., Badizadegan, Kamran, Feld, Michael S., 2006. Optical measurement of cell membrane tension. *Phys. Rev. Lett.* 97 (21), 218101.
- Rincon, Mercedes, 2012. Interleukin-6: from an inflammatory marker to a target for inflammatory diseases. *Trends Immunol.* 33 (11), 571–577.
- Sen, Dipankar, Gilbert, Walter, 1990. A sodium-potassium switch in the formation of Four-stranded G4-DNA. *Nature* 344 (6265), 410–414.
- Sidorenko, Svetlana, Klimanova, Elizaveta, Milovanova, Kseniya, Lopina, Olga D., Kapilevich, Leonid V., Chibalin, Alexander V., Orlov, Sergei N., 2018. Transcriptomic changes in C2C12 myotubes triggered by electrical stimulation: role of Ca²⁺-mediated and Ca²⁺-independent signaling and elevated [Na⁺]_i/[K⁺]_i ratio. *Cell Calcium* 76 (December), 72–86.
- Skou, J.C., Esmann, M., 1992. The Na,K-ATPase. *J. Bioenerg. Biomembr.* 24 (3), 249–261.
- Therien, Alex G., Nestor, Nestor B., Ball, William J., Blostein, Rhoda, 1996. Tissue-specific versus isoform-specific differences in cation activation kinetics of the Na,K-ATPase (*). *J. Biol. Chem.* 271 (12), 7104–7112.
- Turlier, Hervé, Betz, Timo, 2018. Fluctuations in Active Membranes. *ArXiv:1801.00176 [Physics]*, October. <http://arxiv.org/abs/1801.00176>.
- Vakhrusheva, Anna, Endzhiyevskaya, Sofia, Zhukov, Vsevolod, Nekrasova, Tatyana, Parshina, Evgenia, Ovsiannikova, Natalia, Popov, Vladimir, Bagrov, Dmitry, Minin, Alexander A., Sokolova, Olga S., 2019. The role of Vimentin in directional migration of rat Fibroblasts. *Cytoskeleton* 76 (9–10), 467–476.
- Vandesompele, Jo, De Preter, Kathleen, Pattyn, Filip, Poppe, Bruce, Van Roy, Nadine, De Paepe, Anne, Frank, Speleman, 2002. Accurate normalization of real-time quantitative RT-PCR data by geometric averaging of multiple internal control genes. *Genome Biol.* 3 (7) research0034.1.
- Su, Wang, Fei, Meng, Sindu, Mohan, Bipin, Champaneri, Yuchun, Gu, 2009. Functional ENaC channels expressed in endothelial cells: a new candidate for mediating shear force. *Microcirculation* 16 (3), 276–287.
- Wardener, Hugh E. de, Sagnella, Giuseppe A., He, Feng J., MacGregor, Graham A., Markandu, Nirmala D., 2004. Plasma sodium: ignored and underestimated. *Hypertension* 45 (1), 98–102.
- Wardener, H. E. de, MacGregor, G.A., Schillers, H., Riethmüller, C., Hausberg, M., Oberleithner, H., 2007. Plasma sodium stiffens vascular endothelium and reduces nitric oxide release. *Proc. Natl. Acad. Sci. Unit. States Am.* 104 (41), 16281–16286.
- Weik, Christian, Ulrich, Warskulat, Bode, Johannes, Peters-Regehr, Thorsten, Häussinger, Dieter, 1998. Compatible organic osmolytes in rat liver sinusoidal endothelial cells. *Hepatology* 27 (2), 569–575.
- Wenzel, Ulrich O., Bode, Marlies, Kurts, Christian, Ehmke, Heimo, 2019. Salt, inflammation, IL-17 and hypertension. *Br. J. Pharmacol.* 176 (12), 1853–1863.
- Wild, J., Soehnlein, O., Diemel, B., Urschel, K., Garlisch, C.D., Cicha, I., 2014. Rubbing salt into wounded endothelium: sodium potentiates proatherogenic effects of TNF-α under non-uniform shear stress. *Thromb. Haemostasis* 112 (1), 183–195.
- Woo, Seung Kyoon, Dahl, Stephen C., Handler, Joseph S., Moo Kwon, H., 2000. Bidirectional regulation of tonicity-responsive enhancer binding protein in response to changes in tonicity. *Am. J. Physiol. Ren. Physiol.* 278 (6), F1006–F1012.
- Xu, Wei, , Seok Jong Hong, Zhong, Aimei, Xie, Ping, Jia, Shengxian, Xie, Zhong, Zeitchek, Michael, et al., 2015. Sodium channel Nax is a regulator in epithelial sodium homeostasis. *Sci. Transl. Med.* 7 (312), 312ra177–312ra177.
- Yusipovich, A.I., Parshina, E. Yu., Brysgalova, N. Yu., Brazhe, A.R., Brazhe, N.A., Lomakin, A.G., Levin, G.G., Maksimov, G.V., 2009. Laser interference microscopy in erythrocyte study. *J. Appl. Phys.* 105 (10), 102037.